A Simple Multibody 2d-model for Early Postural Checks in Workplace Design

International Journal of Applied Engineering Research ISSN 0973-4562 Volume 12, Number 23 (2017) pp. 14451-14461

A Simple Multibody 2d-model for Early Postural Checks in Workplace Design

Raffaele Castellone[1,*], Stefania Spada[2], Fabrizio Sessa[3] and Maria Pia Cavatorta[1,&]

[1] Department of Mechanical and Aerospace Engineering, Politecnico di Torino, Corso Duca degli Abruzzi, 24, 10129, Torino, Italy.
[2] FCA, Manufacturing Planning & Control – Ergonomics, Corso Settembrini 53, 10135, Torino, Italy.
[3] FCA, Manufacturing Engineering Southern Italy, Pomigliano d'Arco (NA), Italy.

[*]Orcid: 0000-0003-3453-0264, [&]Orcid: 0000-0002-1569-1444
**Corresponding Author's email : raffaele.castellone@polito.it*

Abstract

Posture prediction is one of the most important aspects of virtual modeling tools used for the workplace design: once the work point to reach is defined, the posture prediction module allows simulating, through inverse kinematics, the posture the operator is likely to assume. The paper presents a simple multibody 2D-model created for early postural checks in the design phase. The tool is a spreadsheet created in Microsoft Excel environment, with the support of Visual Basic. The principal output of the model in terms of angles of trunk bending and upper arm elevation, set in compliance with the technical standards, are compared to the results of an established software tool for ergonomic analyses, the 3D Static Strength Prediction Program (3DSSPP). Finally, possible differences in terms of moments on the L5/S1 and the shoulder joints introduced by the simplified kinematics of the 2D manikin are discussed.

Keywords: Digital Human Modeling (DHM), work design, ergonomics of workplace, computer-aided design, biomechanical investigation, proactive ergonomics

INTRODUCTION

Proactive ergonomics emphasizes primary prevention of musculoskeletal disorders (MSD) through recognition and mitigation of risk factors in the design and industrialization stages of new work processes. Ergonomic assessments, such as joint stress analyses and worker's postural demand and discomfort, can be conducted before the workplace and the task even exist by inserting a digital human model (DHM) into a virtual representation of the work environment.

DHM programs are increasingly being used to effectively shorten design- to- build time and costs [1], but also because was demonstrated that DHM simulations provide good estimations of the workload in real-life tasks [2]. Several software packages have been developed in recent years and different studies have proposed a classification according to specific criteria for their use in the design phase [3]. The software programs differ in their complexity, features, and field of application, but also for the quality and accuracy of the results. An initial distinction can be made depending on the complexity of the kinematic model at the basis of the virtual manikin. The multibody manikins are kinematic chains constituted by rigid segments (body parts), linked by joints characterized by multiple degrees of freedom (d.o.f.) (articular joints). In the most complete and accurate software programs, joints generally have all d.o.f. exhibited by the corresponding natural joint, but a longer time is required to prepare the simulation (pre-processing) and for the solution phase. Other software programs use a simpler kinematic model, characterized by a limited number of d.o.f. for some of the joints, allowing for shorter pre-processing and solution times. These easier models may be preferable in industrial applications, especially for early checks in the design phase. One of the goals of this paper is to investigate whether a simple planar model, with a limited number of d.o.f., can predict, with reasonable accuracy, the postural cost associated to different working points in the reachability area in front of the manikin.

Recently, the differences due to the replication of the posture in DHM programs observed from photos or videos of real subjects were quantified [4]. These differences are often not negligible. Therefore, the posture prediction algorithms represent a method that is unaffected by this kind of error. Posture prediction is one of the main applications of virtual modeling tools: once the work point to reach is defined, the posture prediction module allows simulating, through inverse kinematics, the posture the operator is most likely to assume. The analyst may then determine the postural angles for the different joints and assess the postural cost of the work activity through comparison with the requirements given in the technical standards (ISO 11226 [5], EN 1005-4 [6]) or by means of risk assessment tools, like OWAS, often implemented in the DHM. The level of complexity of the virtual manikin and the associated d.o.f. for the different joints may influence the predicted posture.

The problem of reachability has been extensively studied by means of experimental tests aimed at the definition of surfaces representative of the maximum reachability of an operator [7], although surfaces are mainly referred to the sitting position, probably because there is a greater field of applications (e.g. reachability in a vehicle). More recently, Sengupta and Das [8] carried out experimental tests of reachability on subjects grouped by gender with both upright standing and seated postures, in order to obtain maximum reachability curves for different percentiles. Experimental tests on real subjects can be statistically analyzed to develop various predictive models of posture; this approach is called empirical-statistical modeling. These models have been implemented in several software programs. For example, the 3D Static Strength Prediction Program™ (3DSSPP) refers to the empirical-statistical model developed by Beck and Chaffin [9]. 3DSSPP is considered a reference model in the literature and will be used as the basis for comparison in this work.

Other DHM tools implement a postural prediction module based on inverse kinematics algorithms. The motion of the rigid segments is mathematically modeled in order to formulate a set of equations that can be solved to calculate the joint angles. Abdel-Malek et al. presented an overview of these methods [10]. Delangle et al. [11] in their study evaluated the differences between numerical methods and experiments for reachability tests.

The inverse kinematic approach was already used in the work of Ryan et al. [12] for carrying out a simulation of the reachability of pilots within a cockpit. The use of objective functions has improved these models and the prediction of postures has become more realistic [13]. The simple software program presented in the paper has been developed using inverse kinematics algorithms based on the geometrical compliance of the body linked segments in the sagittal plane.

A simple virtual manikin, with a limited number of d.o.f. and the kinematics constrained in the sagittal plane, has already been used for simulations of reachability [12]. In their work, the authors defined envelope surfaces that are representative of the maximum reachability in space, for a given value of the manikin's trunk bending. In particular, three surfaces related to the maximum reachability in space for the conditions of 0, 30 and 60 degrees of trunk bending were obtained. However, these curves do not allow for evaluating the amount of trunk bending for working points inside the area of reachability.

The aim of this work is to provide indications on the postural cost associated with working points within the reachability area in front of the manikin and to compare the posture predicted by two virtual modeling tools characterized by a different degree of complexity of the manikin kinematics and a different approach for solving the redundancy of the kinematic problem. The comparison looks at the angles of trunk bending and upper arm elevation and at the postural assessments, based on traffic light evaluations, in compliance with the requirements of the ISO 11226 [5] and UNI EN 1005/4 [6] technical standards.

As a second objective, the work investigates the effect of the simulated posture on the biomechanical analysis of joint reaction moments and the percentage of the strength capability. Experimental studies have extensively shown that posture influences the force exertion [15, 16; 17; 18]. More recently, using the experimental data, equations to predict arm strength based on hand location and arm posture were obtained [19]. La Delfa and Potvin [20] also studied the relationship among arm strength, shoulder moment and arm posture, researching postures and force directions where arm strength can be maximized. The arm strength depends on the joint strength and consequently, the posture also affects the strength capability in the articular joints. In fact, the equations based on experimental studies of the forces with different postures [21, 22, 23] have been implemented in many DHM programs in order to assess the percent capable (the percentage of the population with the strength capability to generate a moment larger than the resultant moment).

MATERIAL AND METHODS

The first step of this work was mapping the trunk and upper arm elevation postural angles obtained from the virtual simulation of reachability operations. The software programs used for this purpose are 3DSSPP of the University of Michigan, and a program called Human Model (HM), that Fiat Chrysler Automobiles (FCA) developed for early checks in the design phase in cooperation with the academia. HM is indeed a fast and simple tool that can run on a widespread program like Excel and can be used by ergonomists that are inexperienced at virtual modeling. Traffic light evaluations, set in compliance with the technical standards, guide the ergonomist through the early design checks.

The two software programs

The 3DSSPP program is particularly suitable to analyze movements and postures during tasks of manual material handling (MMH). More specifically, it has been developed to simulate static postures or slow movements (assuming that the effects due to acceleration are negligible). 3DSSPP has two options of use: the first consists of setting postural angles as input data to place the manikin in the desired position (direct kinematics), the second option (inverse kinematics) allows to predict the posture assumed by the manikin by inputting the coordinates of the point to reach with the hands. In particular, it allows estimating the posture that a person is likely to assume during a reachability task. However, the estimated posture may not be the posture that every person tends to assume due to physical, behavioral and training differences between individuals [24]. The virtual manikin of 3DSSPP is an advanced biomechanical "top-down" model, which permits the computation of all the forces and moments applied in each joint of the model. The model, starting from the hand loads, solves

the static equilibrium and calculates all the joint reactions up to the ground reaction forces [25].

HM is used in FCA in the early design phase of the workstations on the production line, for its usability and quickness in obtaining initial feedbacks. Differently from 3DSSPP, HM is a simple multibody 2D-model, where each body segment is modeled by a rigid segment of given length and zero mass and it is connected to the adjacent segments by means of joints. Each joint has a number of d.o.f that depends on the movements allowed for the joint. More specifically, the pelvis and the shoulder are modeled as spherical joints, characterized by three d.o.f., whereas the elbow has one d.o.f. only [26]. The kinematics of the anthropometric manikin has a hierarchical structure of nodes. The primary node is the pelvic joint, called root, whereas the others joints are derived nodes; this means that a rotation of the "father" joint causes the rotation of all "son" joints, on the contrary, a rotation of any "son" joint has no impact on the "father" joint [27]. In addition to the direct kinematics, it is also possible to use the inverse kinematics with a reduced number of d.o.f.: bending of the trunk, front elevation of the arm and elbow flexion. This simplification allows to simulate postures in a plane parallel to the sagittal plane and to identify the point to reach with two coordinates (Z= vertical height from floor and Y= horizontal distance from the frontal plane). The X coordinate of the point is relative to the distance of the working point from the sagittal plane; it is automatically set to the value of the X coordinate of the elbow for the anthropometric percentile used to create the manikin.

In order to keep the inverse kinematic problem with a univocal solution, the posture prediction algorithm estimates the posture of the manikin according to two conditions (Figure 1-2):

1. If the operating point is within the reachability area of the manikin arm, the manikin trunk is kept upright and the point is reached through rotation of the shoulder and elbow joints (γ and θ angle, respectively, in Figure 1) (Kinematic condition 1).
2. If the operating point is further away, the arm is kept extended and the point is reached through the rotation of the pelvic joint, i.e. causing trunk bending, and of the shoulder joint (θ and α angle, respectively, in Figure 2) (Kinematic condition 2).

Figures 1-2 show the graphic interface of the HM environment with the front and side views of the manikin and their reference system. The front views show half manikin for symmetry with respect to the sagittal plane.

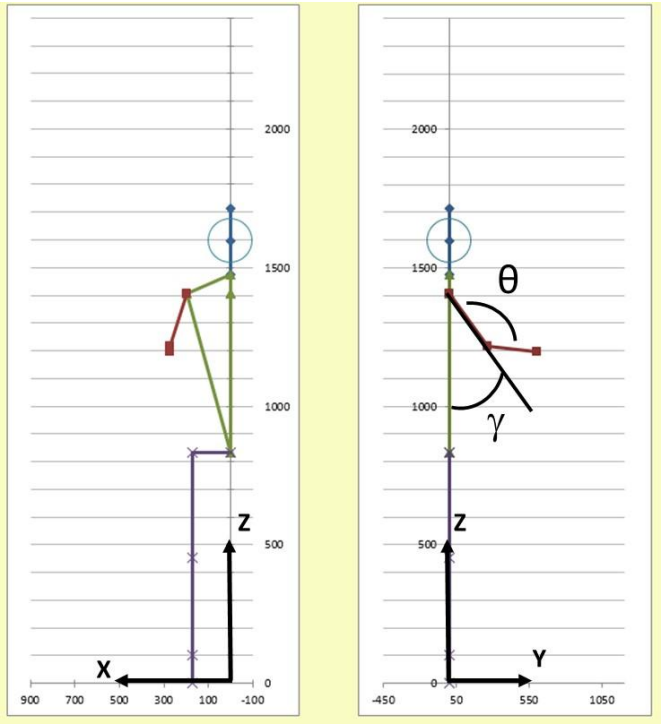

Figure 1: Front and side views of the HM graphic interface. The manikin's posture is in Kinematic condition 1, γ is the upper arm elevation angle and θ is the elbow flexion angle.

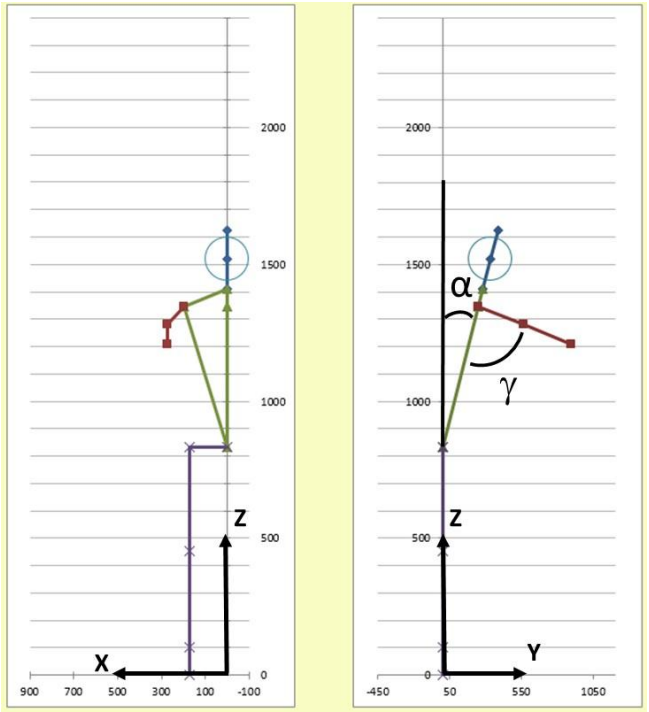

Figure 2: Front and side views of the HM graphic interface. The manikin's posture is in Kinematic condition 2, α is the trunk bending angle and γ is the upper arm elevation angle

Anthropometric model

The 3DSSPP and HM programs make use of different anthropometric databases: 3DSSPP is based on National Health and Nutrition Examination Survey (NHANES), a study on the US civilian population, while the HM refers to the international technical standards ISO 7250-1 [28] and ISO 7250-2 [29] using populations of interest. In both the software programs, the user can select the anthropometry of the virtual manikin by setting the gender and, in the case of HM, the population of interest, and by choosing a percentile among P5, P50, and P95. In addition, 3DSSPP allows the creation of a customized manikin through "scaling" techniques, using height and weight as input parameters. In the present work, we selected the P50 Italian male in HM, while a "scaled manikin" was created in 3DSSPP using the height and weight of the P50 Italian male selected for the HM, thus to minimize anthropometric differences between manikins.

The reachability space

In order to map postural angles, we carried out several reachability tests with both programs. In inverse kinematics, the HM prediction tool works on planes parallel to the sagittal plane. For the comparison, in both the programs the X coordinate was set at 200 mm, which represents a point aligned with the elbow joint of the manikin. The reachability area, in the plane X = 200 mm, was vertically delimited from the hip height (Z = 900 mm) to the full stature of the manikin (Z = 1700 mm). On the other hand, for the horizontal distance Y, the nearest working points were chosen at 200 mm from the frontal plane without considering the body depth, whereas the farthest points (Y = 900mm from the frontal plane) were chosen as limits to possible problems of unbalance. Within the reachability area, a grid of 48 distinct working points was then defined.

The postural angles

For each point on the grid, we performed a simulation with both software programs for predicting the manikin posture in reaching the working point, and then, for each obtained posture we calculated the two postural angles, trunk bending (α) and upper arm elevation (γ), in accordance with the technical standards (ISO 11226, UNI EN 1005-4).

The angle of trunk bending (α) is defined in the sagittal plane, as the inclination of the torso with respect to the vertical axis. In particular, the segment that defines the trunk bending is the line connecting two anthropometric points of the manikin, the greater trochanter to the 7th cervical vertebra.

The upper arm elevation angle (γ) is defined as the elevation of the upper arm during task execution with respect to a reference posture. The segment that defines the elevation of the upper arm is the line connecting two anthropometric points of the manikin, the acromio-clavicular joint to the humeral-radial joint. The calculated angle does not depend on the direction of view during the measurement, but it is the real angle in 3D, while the angle of the reference posture of the arm is 13° from the vertical (ISO 11226 and UNI EN 1005-4).

As anticipated, the HM program is a simplified model with a reduced number of d.o.f. In fact, the inverse kinematics to perform the posture prediction does not evaluate adduction/abduction of the arm, because the X coordinate of the working point is automatically aligned with the elbow joint. For this reason, the upper arm elevation angle (γ) given as output by HM coincides with the angle of front elevation of the upper arm and can be calculated on the sagittal plane.

On the other hand, the 3DSSPP has no limitation on the number of d.o.f. of the shoulder joint and the arm elevation angle given as output by 3DSSPP is a 3D angle. In this regard, in a second step, we decomposed this 3D angle in the frontal arm elevation angle (measured in the sagittal plane) and the abduction/adduction angle (measured in the frontal plane), in order to investigate the role of the component of abduction/adduction that is neglected in HM.

Simulation settings

The procedures for setting the simulations with the two programs are different because of the differences between the two DHM tools. As anticipated, HM has been designed to get early feedbacks and ergonomic indications: the parameters to be set for the simulations are limited to gender, percentile and coordinates of the point to reach with the hands. In 3DSSPP, in addition to the same input parameters of the HM, it is also possible to define the hand load and the hand position (prone, neutral, supine). In this work, no hand load has been applied and a neutral posture of the hands has been used in order to minimize the differences between the simulations with the two software programs.

The angles of trunk inclination and upper arm elevation were calculated from the predicted postures. These postural angles were compared and analyzed according to the traffic light indications, provided by the international technical standards, to get an “ergonomic cost” for the different postures.

Biomechanical investigation

In addition to the postural analysis, the postures predicted by the two software programs were analyzed and compared as for their influence on biomechanical modeling. In particular, we were interested in understanding whether a simplified kinematics of the manikin could determine a significant variation in the forces and moments computed at the joints. As said, HM is a simple multibody 2D-model that does not allow for calculations of forces and moments on joints, therefore the 3DSSPP was used for this purpose. Predicted postures with HM

were manually inserted in 3DSSPP to run the biomechanical analysis. The anthropometric joints of shoulder, elbow, and hand of the 3DSSPP "scaled manikin" were set to coincide with the location predicted by the HM with a tolerance of ± 10 mm. To validate the procedure, working points with very similar estimated postures from the two programs were first analyzed, in order to quantify the differences, if any, in the calculation of the biomechanical load due to the manual insertion of the HM posture in the 3DSSPP.

A force of 90N was applied on the right hand in the downward direction parallel to the vertical axis to simulate a lifting of a weight of approximately 9 Kg. Moments on the shoulder and L5/S1 joints were then calculated for different points to reach, for both the HM and 3DSSPP predicted postures.

RESULTS AND DISCUSSIONS

Trunk bending (α angle)

Tables 1-2 report the values for the angle of trunk bending (α) for the obtained postures in the reachability simulations carried out with HM and 3DSSPP. In order to compare the values, it was necessary to calculate the output angles of the two programs in the same reference system. In both tables, cells are colored in accordance with the technical standards (ISO 11226 and UNI EN 1005/4), with a traffic light evaluation corresponding to the following ranges of angular values:

- $0° \leq \alpha < 20°$ acceptable condition (green)
- $\alpha < 0°$, $20° \leq \alpha < 60°$ condition to be verified (yellow)
- $\alpha \geq 60°$ unacceptable condition (red)

Table 1: Angular values (°) and their traffic light assessment for the trunk bending angle in reachability tests using HM. Y and Z (mm) are the coordinates of the working point to reach.

	HM							
	Y=200	Y=300	Y=400	Y=500	Y=600	Y=700	Y=800	Y=900
Z=1700	0	0	0	0	1	11	24	NR
Z=1550	0	0	0	0	0	5	16	29
Z=1400	0	0	0	0	0	4	14	25
Z=1200	0	0	0	0	0	7	17	26
Z=1100	0	0	0	0	1	11	20	29
Z=900	0	0	0	7	15	23	31	39

Table 2. Angular values (°) and their traffic light assessment for the trunk bending angle in reachability tests using 3DSSPP. Y and Z (mm) are the coordinates of the working point to reach.

	3DSSPP							
	Y=200	Y=300	Y=400	Y=500	Y=600	Y=700	Y=800	Y=900
Z=1700	0	0	1	4	7	15	33	NR
Z=1550	0	1	3	5	7	11	21	39
Z=1400	2	3	5	6	9	12	18	30
Z=1200	5	6	8	10	12	15	21	33
Z=1100	7	8	10	11	14	17	24	36
Z=900	11	12	14	16	19	27	36	45

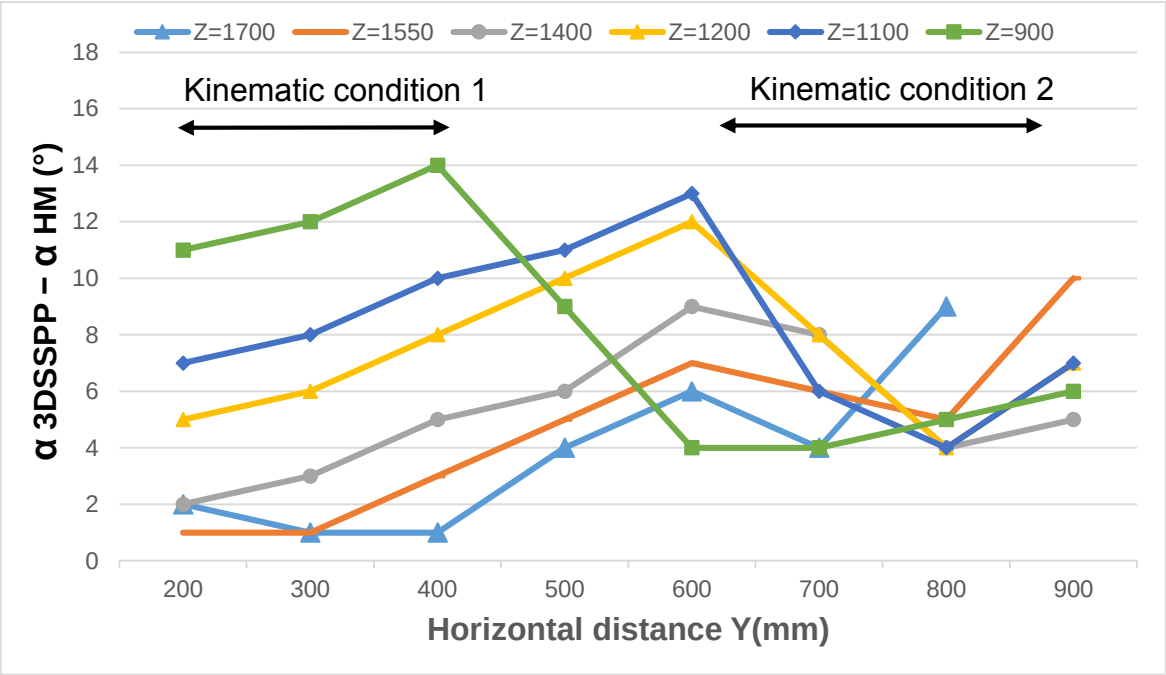

Figure 3: The difference in the trunk bending angle calculated with the two programs

Out of the 48 points to reach that were selected for the simulations, only the farthest point of the grid (Y=900 mm, Z=1700 mm) is not reachable (NR). Angular values for trunk bending predicted by HM are generally smaller. However, when considering the traffic light evaluation, the comparison between Table 1 and Table 2 shows that, only in 2 cases out of 47, the traffic light evaluation associated with the posture predicted by the two programs is different: green for HM and yellow for 3DSPP. In both cases, the angle value for 3DSSPP is 21°, a value very close to the threshold that separates the green and yellow region.

The difference in the angle of trunk bending predicted by the two programs ($\alpha_{3DSSPP} - \alpha_{HM}$) was calculated for all points of the grid. The mean difference for each grid point is 6.3° with a standard deviation of 3.3°. The six curves in Figure 3 outline ($\alpha_{3DSSPP} - \alpha_{HM}$) with respect to the horizontal distance from the body of the point to reach, at various vertical heights from floor. The horizontal distances for which the HM manikin estimated posture belongs to the first or second kinematic condition are indicated in the graph. In the intermediate area, both conditions are possible depending on the vertical height from floor.

As it can be seen in Figure 3, the largest difference in the predicted trunk bending angle, throughout the reachability area, is 14°, with only 6 cases out of 47 showing a difference in the predicted angle larger than 10°. When the point to reach is close to the body, the posture predicted by HM is an upright posture (constrained by kinematic condition 1). The posture predicted by 3DSSPP is based on a postural database and it is characterized by bending of the trunk even when the working point can be reached otherwise, likely to ensure better visibility of the point to reach and the capability to exert greater forces. In fact, especially the work points close to waist level show a greater error. In addition, the difference between the predicted trunk bending angle grows as the horizontal distance increases up to the point of transition to kinematic condition 2. For working points in kinematic condition 2, all the curves tend to similar and smaller values of difference. As the horizontal distance of the working point increases further, and the limit of reachability is approached, the postures predicted by 3DSSPP are again characterized by a greater degree of trunk bending, likely to ensure better visibility and to enable greater forces.

Upper arm elevation (γ angle)

Tables 3 and 4 report the angles of the upper arm elevation (γ). Similarly to Tables 1-2, cells are colored in accordance with the indications provided in the technical standards ISO 11226 and UNI EN 1005/4:

- $0° \leq \gamma < 20°$acceptable condition (green)
- $20° \leq \gamma < 60°$ condition to be verified (yellow)
- $\gamma \geq 60°$ unacceptable condition (red)

Table 3: Angular values (°) and their traffic light assessment for the upper arm elevation angle in reachability tests using HM. Y and Z (mm) are the coordinates of the working point to reach.

	HM							
	Y=200	Y=300	Y=400	Y=500	Y=600	Y=700	Y=800	Y=900
Z=1700	86	82	84	91	117	129	146	NR
Z=1550	54	54	58	67	82	108	121	138
Z=1400	12	23	35	47	64	93	105	119
Z=1200	EXT.	EXT.	14	31	54	79	91	104
Z=1100	EXT.	EXT.	11	30	64	74	86	99
Z=900	EXT.	3	25	48	58	69	81	94

Table 4: Angular values (°) and their traffic light assessment for the upper arm elevation angle in reachability tests using 3DSSPP. Y and Z (mm) are the coordinates of the working point to reach.

	3DSSPP							
	Y=200	Y=300	Y=400	Y=500	Y=600	Y=700	Y=800	Y=900
Z=1700	90	84	84	89	99	118	146	NR
Z=1550	64	61	64	69	78	92	112	140
Z=1400	32	37	45	52	63	76	94	116
Z=1200	EXT.	EXT.	28	37	48	62	80	98
Z=1100	EXT.	EXT.	24	32	44	58	77	93
Z=900	EXT.	13	18	29	46	60	74	94

Standards also recommend avoiding awkward postures for the upper limb that include particular movements as extension, adduction, and external rotation. The postures that require an extension of the arm are indicated as (EXT) and are considered unacceptable.

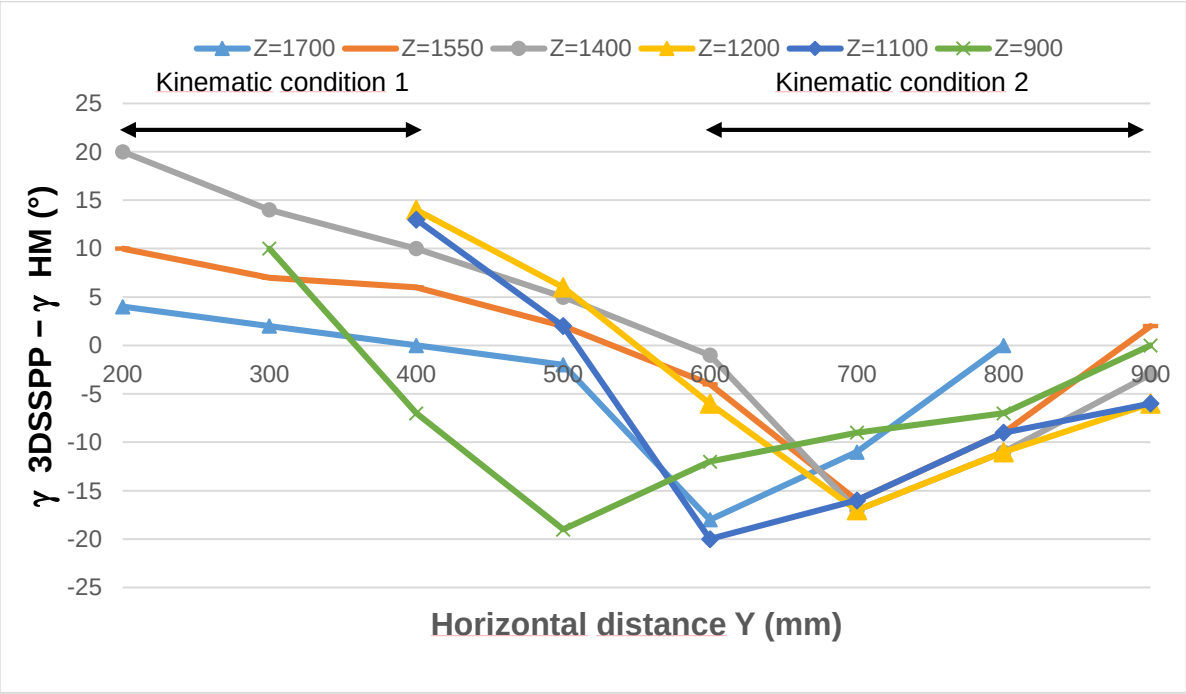

Figure 4: The difference in the upper arm elevation angle calculated with the two programs

The comparison of colors between Tables 3 and 4 shows that in 36 cases out of 47 the traffic light indications match. For the 9 cases for which there is no color matching, it is worthwhile noticing that the absence of the d.o.f. of arm abduction in the HM determines the underestimation of the real 3D upper arm elevation angle for working points close to the body (Y< 400 mm). For points more distant from the body, on the contrary, the kinematic conditions 2 of arm extended leads to an overestimation of the upper arm elevation angle. Computation of the absolute value of the difference in the predicted arm elevation angle $|\gamma_{3DSSPP} - \gamma_{HM}|$ shows a mean difference of 9.0° with a standard deviation of 5.9°. Similarly to Figure 3, Figure 4 depicts the value of the difference $(\gamma_{3DSSPP} - \gamma_{HM})$ with respect to the horizontal distance at the different vertical heights. Work points where the predicted postures require extension of the arm were excluded. All curves exhibit a similar trend.

Under kinematic condition 1, the absence of the d.o.f. for shoulder abduction/adduction implies that in HM the arm is constrained to move within a plane and it is possible for the manikin to reach working points at around waist level with a lower angle of upper arm elevation. As the horizontal distance of the working point increases, the component of arm abduction reduces and the difference between the two predicted postures diminishes. Figure 5 shows the reduction of the component of shoulder abduction as the horizontal distance from the body of the point to reach increases, at various vertical heights from the floor. The abduction angle was computed from the 3D angle of 3DSSPP as illustrated in Section 2.4.

The transition from kinematic condition 1 to kinematic condition 2 is the reason for the sharp increase in the difference between the predicted angles: the HM manikin in kinematic condition 2 reaches the working point with the arms extended. As the horizontal distance of the working point increases further, the posture with the arms extended simulated by the HM resembles more the postures predicted by 3DSSPP.

Biomechanical analysis

3DSSPP was used to investigate the biomechanics of the postures predicted by the two software programs. Table 5 shows the results for the three working points that exhibit the highest differences in terms of predicted angles for trunk bending (α) and upper arm elevation (γ). The reported moments on the L5/S1 ($M_{L5/S1}$) and shoulder joints (M_s) represent the moments of flexion/extension of the joints. For both the L5/S1 and shoulder joints, flexion/extension is the most critical component of the vector moment for the type of kinematics that characterizes the 2D model implemented in the HM program. The percentage difference of the moments (ε_M= (M_{HM}-M_{3DSSPP}) /M_{3DSSPP}) was calculated for the L5/S1 ($\varepsilon_{ML5/S1}$) and shoulder joints (ε_{MS}) respectively. Table 5 also reports the values of the mean strength and its standard deviation (SD) for the reference population as provided by the 3DSSPP strength database and the associated percent capable, which quantifies the population that is able to support the load on the joint (University of Michigan, 1995).

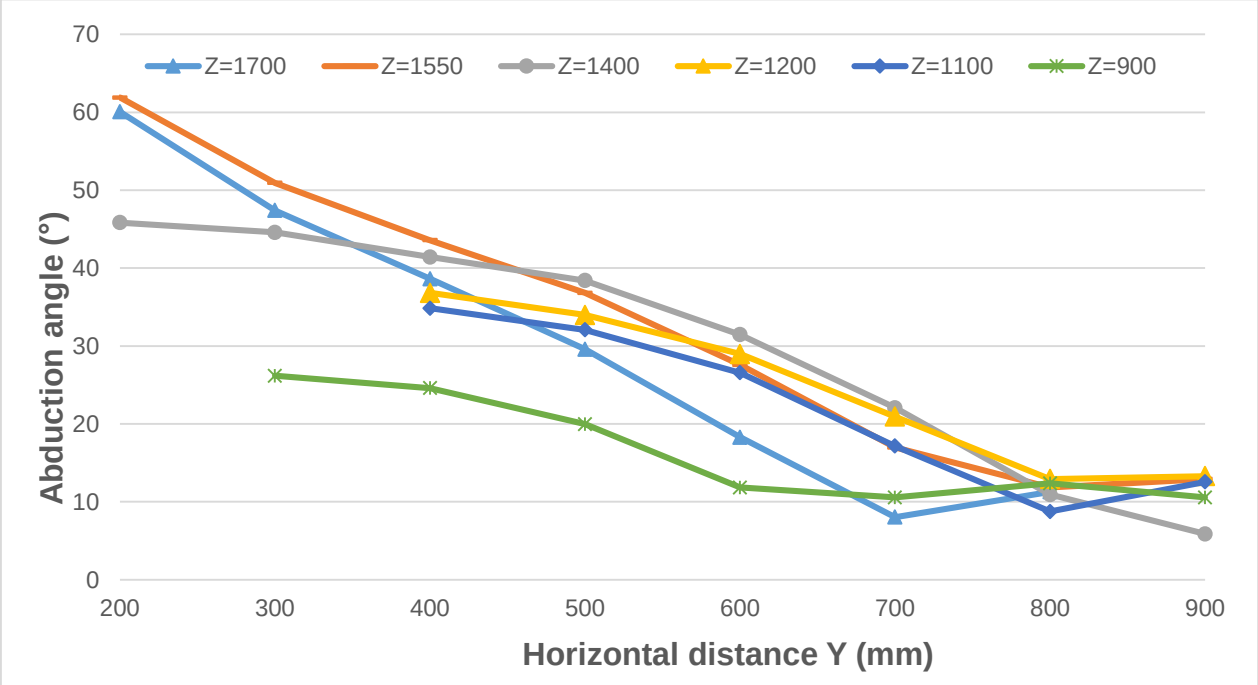

Figure 5: The abduction angle vs. the horizontal distance of the working point to reach at various vertical height from floor

Table 5: Posture angles (°), flexion/extension moments (Nm) and percentage differences of the L5/S1 and shoulder joints. All compared to the Mean, SD of the population strength and Percent capable (Cap).

				L5/S1 (Flex/Ext)					**Shoulder (Flex/Ext)**				
				Required		Population strength			Required		Population strength		
Work point (mm)	Posture	α (°)	γ (°)	$M_{L5/S1}$ (Nm)	$\varepsilon M_{L5/S1}$ (%)	Mean (Nm)	SD	Cap (%)	M_S (Nm)	εM_S (%)	Mean (Nm)	SD	Cap (%)
Y=400, Z=900	HM	0	25	50	-44%	220	69	99	43	59%	77	19	96
	3DSSPP	14	18	90		254	80	97	27		72	18	99
Y=600, Z=1100	HM	1	64	80	-30%	223	70	97	65	38%	78	19	74
	3DSSPP	14	44	115		250	79	96	47		71	17	91
Y=600, Z=1200	HM	0	54	78	-30%	220	69	97	68	33%	77	19	69
	3DSSPP	12	48	111		247	78	96	51		70	17	87

As expected, $\varepsilon_{ML5/S1}$ is always negative because of the smaller trunk bending (α) predicted by HM. For increasing trunk bending, there is an increase in the component of the trunk weight that is accounted for in the equilibrium equation. The moments computed for the three HM postures were found to be 30-44 % lower than the corresponding values for the 3DSSPP postures.

On the other hand, Table 5 shows positive ε_{MS} values for all three analyzed working points. In the HM posture, the lower trunk bending determines a greater distance between the shoulder joint and the hand, leading to an overestimation of the calculated moment. For the working point (Y = 400, Z= 900) the difference in the calculated moment is almost 60%.

Even though the percentage differences may seem large, the percent capable evaluated for the two predicted postures do not carry significant differences when it comes to the L5/S1 joint. The computed moments are relatively small when compared to the mean strength values. At the tail of the Gaussian distribution, large variations in the moment are needed to determine a significant change in the strength percentile.

For the shoulder joint, a larger difference in the percent capable, evaluated for the two predicted postures, is associated with the two working points at Y=600, even though these points are not characterized by the largest percentage differences in the computed moments. As the lever arm of the applied force increases, the moment on the shoulder joint enlarges. Moving away from the tail of the Gaussian distribution, differences in the computed moment have a larger impact on the strength percentile associated with them. Quite obviously, the applied external load influences the calculated moments and the percent capable. Additional simulations were run for the same working points by varying the load applied at the hand. The percentage difference for the calculated moment on the two joints did not vary, while the change in the percent capable had a lesser or greater effect depending on the level of the computed moment with respect to the mean value of the population strength. More specifically, the closer the calculated moment is to the mean value of the population strength distribution, the larger is the impact on the percent capable for a given difference in moment. Conversely, the effect on the evaluation of the percent capable lessens when analyzing the tails of the strength distribution.

As said, Table 5 reports the biomechanical analysis of the three postures that exhibit substantial postural differences. However, in all cases the HM program overestimates the upper arm elevation angles. It was therefore decided to analyze other working points in order to complete and deepen the biomechanical investigation.

Table 6: Posture angles (°), flexion/extension moments (Nm) and percentage differences of the L5/S1 and shoulder joints. All compared to the Mean, SD of the population strength and Percent capable (Cap).

				L5/S1 (Flex/Ext)					**Shoulder (Flex/Ext)**				
				Required		Population strength			Required		Population strength		
Work point (mm)	Posture	α (°)	γ (°)	$M_{L5/S1}$ (Nm)	$\varepsilon M_{L5/S1}$ (%)	Mean (Nm)	SD	Cap (%)	M_S (Nm)	εM_S (%)	Mean (Nm)	SD	Cap (%)
Y=200, Z=1400	HM	0	12	27	0%	220	69	99	19	46%	64	16	99
	3DSSPP	5	32	27		225	71	99	13		77	19	99
Y=400, Z=1100	HM	0	11	48	-36%	220	69	99	36	64%	72	18	97
	3DSSPP	10	24	75		243	77	98	22		64	16	99
Y=400, Z=1550	HM	0	58	56	-8%	220	69	99	48	30%	71	18	90
	3DSSPP	3	64	61		227	72	89	37		65	16	95

In particular, Table 6 shows the biomechanical analysis of three working points in which the HM underestimates the trunk bending as well as the upper arm elevation, providing, for the latter angle, a different traffic light indication. In line with Table 5, the percentage difference $\varepsilon M_{L5/S1}$ is always negative. On the contrary, despite the smaller angle of the upper arm elevation, εM_S is still positive, meaning that higher values of the shoulder joint moment were calculated for the posture predicted by HM. These results confirm that the calculated moment on the shoulder joint is mainly related to the trunk bending, and consequently to the distance between the shoulder joint and the hand.

It is also important to note that a significant limitation of the static strength demand approach used in many DHM software programs, including 3DSSPP, is that they consider the individual strength axes of the shoulder as independent [30]. They evaluate the strength capable based on the highest component of the vector moment (the flexion/extension in the sagittal plane in this work). This analysis is well suited for the HM model kinematics, where the components of abduction/adduction and of humeral rotation are negligible when compared to flexion/extension. On the other hand, for the postures predicted by the 3DSSPP program, the moment components of abduction and humeral rotation can be comparable to that of flexion/extension, particularly for working points close to the body where shoulder abduction is significant (Figure 5). When calculating the resultant vector moment on the shoulder joint, the percentage difference between the postures predicted by HM and 3DSSPP decreases significantly. In line with Hodder et al. [30], more accurate and conservative assessments can be achieved when the DHM software considers the combined contribution of the calculated moments in the different axes of the shoulder joint.

Although this analysis is limited to one load direction only, results show that 2D manikins can be useful for quick evaluations in the first phase of design even when the predicted posture is used for biomechanical assessments. Further investigations with other hand loads and load directions could support and integrate these initial results.

CONCLUSIONS

The comparison with a reference literature model like 3DSSPP showed that a simple 2D manikin, with a limited d.o.f. and the kinematics constrained in the sagittal plane, could provide useful and reliable indications to assist the design phase. The results acquire a greater value when considering that this simple model runs on a widespread program like Excel and can be used by ergonomists that are inexperienced at virtual modeling.

Tables of trunk bending and upper arm elevation angles, in the reachability area in front of the manikin, provide important information on the "postural cost" associated with the predicted postures. Traffic light indications, associated to the angular values in compliance with the international technical standards, may support the ergonomist in early checks during the design phase.

The biomechanical analysis run on the postures predicted by the two programs confirmed the importance of an accurate posture prediction. The static strength demand approach used in many DHM software programs for the strength percent capable determination, in which the individual strength axes of the shoulder are considered as independent, is well suited for manikin kinematics constrained in the sagittal plane, where the components of abduction/adduction and of humeral rotation are negligible when compared to the flexion/extension.

REFERENCES

[1] Chaffin, D. B., 2005, "Improving digital human modelling for proactive ergonomics in design." Ergonomics, 48(5), 478-491.

[2] Fritzsche, L., 2010, “Ergonomics risk assessment with digital human models in car assembly: Simulation versus real life”, Human Factors and Ergonomics in Manufacturing & Service Industries, 20 (4), 287–299.

[3] Poirson, E., and Delangle, M., 2013, “Comparative analysis of human modeling tools”, In International Digital Human Modeling Symposium, Ann Arbor, United States.

[4] Lu, M. L., Waters, T., and Werren, D., 2015, “Development of human posture simulation method for assessing posture angles and spinal loads”, Human Factors and Ergonomics in Manufacturing & Service Industries, 25(1), 123-136

[5] International Standard ISO 11226:2000.: Ergonomics – Evaluation of static working postures.

[6] EN 1005-4:2005+A1, 2008.: Safety of machinery – Human physical performance – Part 4: Evaluation of working postures and movements in relation to machinery.

[7] Bullock, M. I., 1974, “The determination of functional arm reach boundaries for operation of manual controls”, Ergonomics, 17(3), 375-388.

[8] Sengupta, A. K., and Das, B, 2000, “Maximum reach envelope for the seated and standing male and female for industrial workstation design”, Ergonomics, 43(9), 1390-1404.

[9] Beck, D. J., and Chaffin, D. B, 1992, “An evaluation of inverse kinematics models for posture prediction”, Computer Applications in Ergonomics, Occupational safety and health, 329-336.

[10] Abdel-Malek, K., Yu, W., and Jaber, M., 2001, “Realistic posture prediction. SAE Digital Human Modeling and Simulation”

[11] Delangle, M., Petiot, J. F., and Poirson, E., 2016, "Using motion capture to study human standing accessibility: comparison between physical experiment, static model and virtual ergonomic evaluations", International Journal on Interactive Design and Manufacturing (IJIDeM), 1-10.

[12] Ryan, P. W., Springer, W., and Hlastala, M.,1970, "Cockpit geometry evaluation. Joint Army-Navy Aircraft Instrumentation Research Report", 700201.

[13] Jung, E. S., Kee, D., and Chung, M. K., 1995, "Upper body reach posture prediction for ergonomic evaluation models", International Journal of Industrial Ergonomics, 16(2), 95-107.

[14] Parkinson, M. B., and Reed, M. P.,2007, "Standing reach envelopes incorporating anthropometric variance and postural cost", No. 2007-01-2482, SAE Technical Paper.

[15] Chaffin, D. B., Andres, R. O., and Garg, A., 1983, "Volitional postures during maximal push/pull exertions in the sagittal plane", Human Factors: The Journal of the Human Factors and Ergonomics Society, 25(5), 541-550.

[16] Wilkinson, A. T., Pinder, A. D. J., and Grieve, D. W., 1995, "Relationships between one-handed force exertions in all directions and their associated postures", Clinical Biomechanics, 10(1), 21-28.

[17] Roman-Liu, D., and Tokarski, T., 2005, "Upper limb strength in relation to upper limb posture", International Journal of Industrial Ergonomics, 35(1), 19-31.

[18] Chow, A. Y., and Dickerson, C. R.,2009, "Shoulder strength of females while sitting and standing as a function of hand location and force direction", Applied Ergonomics, 40(3), 303-308.

[19] La Delfa, N. J., Freeman, C. C., Petruzzi, C., and Potvin, J. R., 2014, "Equations to predict female manual arm strength based on hand location relative to the shoulder", Ergonomics, 57(2), 254-261.

[20] La Delfa, N. J., and Potvin, J. R., 2016, "Multidirectional manual arm strength and its relationship with resultant shoulder moment and arm posture", Ergonomics, 1-12

[21] Clarke, H. H., 1966, "Muscular Strength and Endurance in Man", Prentice-Hall, Inc., Englewood Cliffs, New Jersey, 39-51.

[22] Stobbe, T. J., 1982, "The development of a practical strength testing program for industry", (Doctoral dissertation, University of Michigan).

[23] Kumar, S., Chaffin, D. B., and Redfern, M., 1988, "Isometric and isokinetic back and arm lifting strengths: device and measurement", Journal of biomechanics, 21(1), 35-44.

[24] The University of Michigan, 2011, "3D Static Strength Predication Program", Ver. 6.0.5, User's Manual, The University of Michigan, Center for Ergonomics, Ann Arbor, Michigan.

[25] Chaffin, D. B., Andersson, G., and Martin, B. J., 1999, Occupational biomechanics, 91-130, New York: Wiley.

[26] Spada, S., Germanà, D., C., Ghibaudo, L., and Sessa, F., 2013, "Applications and benefits of digital human models to improve the design of workcells in car's manufacturing plants according to international standards", Advances in Manufacturing Technology XXVII, 361.

[27] Talamo, L., 2007, "Metodi e strumenti di Digital Human Modeling e Virtual Reality per la progettazione ergonomica di una postazione di lavoro", Dissertation, (in Italian).

[28] International Standard ISO 7250-1:2008: Basic human body measurements for technological design – Part 1: Body measurement definitions and landmarks.

[29] International Standard ISO/TR 7250-2:2009: Basic human body measurements for technological design – Part 2: Statistical summaries of body measurements from individual ISO populations.

[30] Hodder, J. N., La Delfa, N. J., and Potvin, J. R., 2015, "Testing the assumption in ergonomics software that overall shoulder strength can be accurately calculated by treating orthopedic axes as independent", Journal of Electromyography and Kinesiology.